

A PROJECTION OF THE COLD SEASON HYDROCLIMATE IN CALIFORNIA IN MID- TWENTY-FIRST CENTURY UNDER THE SRES-A1B EMISSION SCENARIO

A Paper From:
California Climate Change Center

Prepared By:
**J. Kim, R. Fovell, A. Hall, Q. Li, K. N. Liou,
J. McWilliams, Y. Xue, X. Qu, and S.
Kapnick
University of California, Los Angeles**

**D. Waliser, A. Eldering, Y. Chao, and
R. Friedl
Jet Propulsion Laboratory, California
Institute of Technology**

DISCLAIMER

This paper was prepared as the result of work sponsored by the California Energy Commission (Energy Commission) and the California Environmental Protection Agency (Cal/EPA). It does not necessarily represent the views of the Energy Commission, Cal/EPA, their employees, or the State of California. The Energy Commission, Cal/EPA, the State of California, their employees, contractors, and subcontractors make no warrant, express or implied, and assume no legal liability for the information in this paper; nor does any party represent that the uses of this information will not infringe upon privately owned rights. This paper has not been approved or disapproved by the California Energy Commission or Cal/EPA, nor has the California Energy Commission or Cal/EPA passed upon the accuracy or adequacy of the information in this paper.



Arnold Schwarzenegger, *Governor*



DRAFT PAPER

March 2009
CEC-500-2009-029-D

Acknowledgments

The research described in this paper was performed within the Joint Institute for Regional Earth System Science and Engineering (JIFRESSE), made possible by a Memorandum of Understanding between the University of California, Los Angeles, and the Jet Propulsion Laboratory (JPL), California Institute of Technology, and was sponsored by the National Aeronautics and Space Administration (NASA). Preprocessing of the Community Climate System Model data for this project was also carried out in part by D. Cha and S. Chun who were supported by Grant No. 1700-1737-322-210-13 from the Ministry of Environment, Korea. Computational resources for this study were provided by the JPL Supercomputing and Visualization Facility, as well as the NASA Advanced Supercomputing (NAS) Division.

Preface

The California Energy Commission's Public Interest Energy Research (PIER) Program supports public interest energy research and development that will help improve the quality of life in California by bringing environmentally safe, affordable, and reliable energy services and products to the marketplace.

The PIER Program conducts public interest research, development, and demonstration (RD&D) projects to benefit California's electricity and natural gas ratepayers. The PIER Program strives to conduct the most promising public interest energy research by partnering with RD&D entities, including individuals, businesses, utilities, and public or private research institutions.

PIER funding efforts focus on the following RD&D program areas:

- Buildings End-Use Energy Efficiency
- Energy-Related Environmental Research
- Energy Systems Integration
- Environmentally Preferred Advanced Generation
- Industrial/Agricultural/Water End-Use Energy Efficiency
- Renewable Energy Technologies
- Transportation

In 2003, the California Energy Commission's PIER Program established the **California Climate Change Center** to document climate change research relevant to the states. This center is a virtual organization with core research activities at Scripps Institution of Oceanography and the University of California, Berkeley, complemented by efforts at other research institutions. Priority research areas defined in PIER's five-year Climate Change Research Plan are: monitoring, analysis, and modeling of climate; analysis of options to reduce greenhouse gas emissions; assessment of physical impacts and of adaptation strategies; and analysis of the economic consequences of both climate change impacts and the efforts designed to reduce emissions.

The California Climate Change Center Report Series details ongoing center-sponsored research. As interim project results, the information contained in these reports may change; authors should be contacted for the most recent project results. By providing ready access to this timely research, the center seeks to inform the public and expand dissemination of climate change information, thereby leveraging collaborative efforts and increasing the benefits of this research to California's citizens, environment, and economy.

For more information on the PIER Program, please visit the Energy Commission's website www.energy.ca.gov/pier/ or contact the Energy Commission at (916) 654-5164.

Table of Contents

Preface.....	iii
Abstract	vii
1.0 Introduction.....	1
2.0 Experiment	3
3.0 The Changes in the Low-Level Air Temperature	6
4.0 Precipitation Changes.....	8
5.0 The Changes in the Seasonal Snowpack and Snowmelt.....	11
6.0 Runoff Changes	12
7.0 Summary and Conclusions	13
8.0 References.....	14
9.0 Glossary	16

List of Figures

Figure 1. The cold-season snow-water equivalence (SWE) climatology for the period 1961–1980 in the CCSM3 simulation used to drive the control climate in this study 2

Figure 2. The model terrain (m) of the 36 km resolution western U.S. domain (outer box). The inner box represents the area where the climate signals obtained for this study are presented. The five California sub-regions are marked by colored rectangles..... 4

Figure 3. The information flow in the experiment 5

Figure 4. The CCSM3-projected climate change signals in the (a) low-level air temperature, (b) precipitation, and (c) SWE during the cold season 6

Figure 5. The low-level temperature change signals for: (a) the entire cold season (October–March), (b) fall (October–December: OND), and (c) winter (January–March: JFM) 7

Figure 6. The percent changes in surface albedo for: (a) the entire cold season (October–March), (b) fall (OND), and (c) winter (JFM) 8

Figure 7. The climate change signal in precipitation (percent of the control climate) for: (a) the entire cold season (October–March), (b) fall (OND), and (c) winter (JFM) 10

Figure 8. Same as Figure 5, but for the seasonal rainfall changes 10

Figure 9. Same as Figure 5, but for the seasonal snowfall changes..... 11

Figure 10. The climate change signals (% of the control climate) in SWE for: (a) the entire cold season, (b) fall, and (c) winter 12

List of Tables

Table 1. Precipitation characteristics in the five California sub-regions in Figure 2 4

Table 2. The projected climate change signals in key surface hydrologic variables within the five subregions (Table 1). The numbers in the parenthesis present the climate change in terms of the percent of the late twentieth century RCM climatology. The percent change in snowfall and snowmelt in the southern Coastal Range region (SC) is undefined, due to very small values in both the control and mid-century periods..... 9

Abstract

In this study, researchers performed a projection of the cold season regional climate change signals in the surface hydroclimate fields corresponding to the mid-twenty-first century in California. The projection used the dynamical downscaling method in which a global climate scenario generated by the National Center for Atmospheric Research Community Climate System Model-3 (CCSM-3) is downscaled using a regional climate model, the Weather Research and Forecast model. The global climate scenario is based on the Intergovernmental Panel on Climate Change Special Report on Emission Scenarios (SRES) A1B emission profile. The cold season covers the six-month period October through March, which includes fall (October–December) and winter (January–March). The regional climate change signals are calculated as the differences between the regional climate model climatology for two 20-year periods: the late twentieth century (1961–1980) and the mid-twenty-first century (2035–2054). The results show that the low-level temperature in California will increase by 1°C–2.5°C (1.8°F–4.5°F), with larger increases in high-elevation regions and in winter. Noticeable decreases in snowfall, snow-water equivalent, and surface albedo in high-elevation regions in the projected mid-twenty-first century climate suggest that the temperature increases in the high-elevation regions are partially amplified by local feedback through snow and surface albedo. Precipitation decreases over the entire cold season. The precipitation change signals show well-defined interseasonal variations; a pattern of positive (negative) signals in the northern (southern) California region during fall is reversed in winter. The seasonal variations in the precipitation change pattern are primarily associated with the climate change signals in rainfall. Snowfall decreases in the warmer climate, most noticeably in winter. The changes in seasonal precipitation result in the reduction in snowmelt, seasonal-mean snow-water equivalent, and runoff during the cold season, especially in high-elevation regions. The decrease in the high-elevation snowpack is of a special concern, as it is among the main sources of warm season water supply in California.

Keywords: California climate change, mid-twenty-first century, precipitation, snow-water equivalent, cold season

1.0 Introduction

The impact of the global climate change induced by anthropogenic forcings, especially due to the increase in atmospheric greenhouse gases (GHGs), on the cold season hydroclimate is an important concern for California. Studies on recent climate variability (IPCC 1995, 2007) found that the increase in GHG has already begun altering global and regional climates. The climate of the California region is characterized by extreme contrasts in precipitation with wet cold seasons and dry warm seasons. Moreover, California relies heavily on cold season precipitation for the water supply in the dry warm seasons. Previous studies (e.g., Dettinger and Cayan 1995; Stewart et al. 2005) revealed that global climate change appears to be affecting the snowpack and snowmelt-driven runoff in California's mountainous region. The water supply in California has been marginal for supporting its large population and industries, especially agriculture. Thus, reliable assessments of the impact of the climate change on the future water resources in the region have been an important concern to California's water managers (Anderson et al. 2008).

Existing climate change studies strongly suggest that the water resources in California may be adversely affected by the global climate change induced by the increase in GHGs (Leung and Ghan 1999; Kim 2001, 2004; Kim et al. 2002; Cayan et al. 2008). Details of the regional-scale climate change signals, however, vary among the projections according to emission scenarios, global climate models (GCMs), and regional climate models (RCMs). All projections based on either statistical or dynamical downscaling of various GCM scenarios agree that the increase in the low-level air temperatures and earlier melting of the Sierra Nevada snowpack will occur under higher GHG concentration.

However, significant differences in precipitation exist. For example, the climate change study of Leung and Ghan (1999) on the basis of the dynamical downscaling of a National Center for Atmospheric Research (NCAR) Community Climate Model (CCM3) global climate scenario using the MM5 model projected decreases in winter precipitation in California under the warmer climate condition. On the other hand, the climate change study by Kim et al. (2002) that is based on the dynamical downscaling of the Hadley Centre Climate Model (HadCM2) data using the Mesoscale Atmospheric Simulation (MAS) model, projected increases (decreases) in winter precipitation in northern (southern) California. The differences between these two studies are consistent with the differences in the projected precipitation changes between the two GCMs, at least qualitatively. In fact, regional precipitation changes are among the most uncertain results in the existing global climate change studies (IPCC 2007). The large uncertainties in the projected climate change signals cause difficulties in developing a plan to adapt to and mitigate the impacts of climate change. Despite large uncertainties in the GCM projections, only a limited number of regional climate change studies have been performed for the California region.

Obtaining climate projection data suitable for assessing the impact of climate change on water resources in California has been difficult. Typical resolutions of GCMs that are used to simulate future climate are on the order of 100 kilometers (km). At such a coarse resolution, GCMs cannot account for the effects of regional orography that plays a crucial role in shaping

California's climate (Kim 2001; Kyriakidis et al. 2001; Kim and Lee 2003). One of the problems caused by inadequate representation of orography in simulating surface hydrologic field can be found in the GCM-simulated snow water equivalence (SWE) shown in Figure 1.

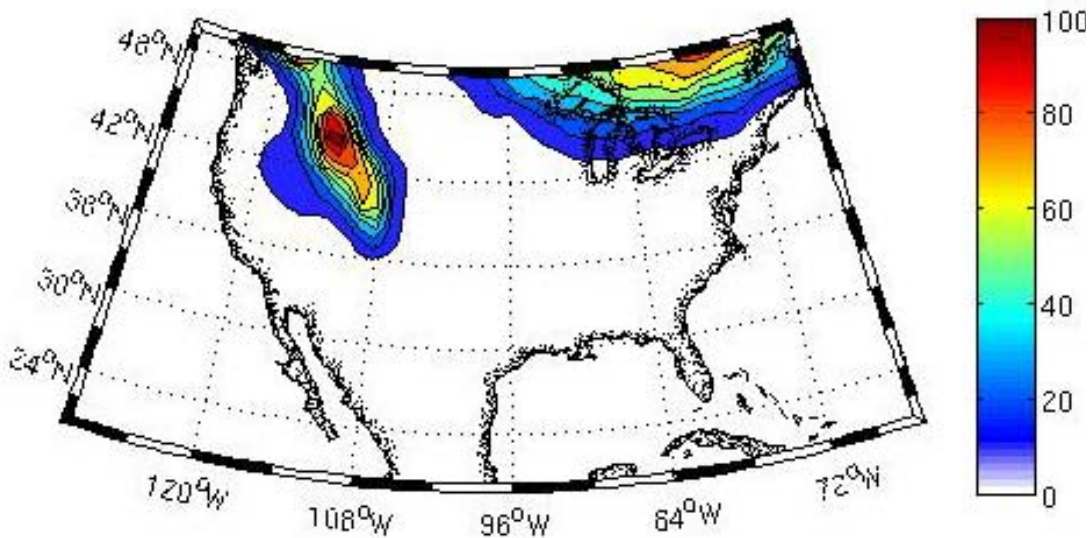


Figure 1. The cold-season snow-water equivalence (SWE) climatology for the period 1961–1980 in the CCSM3 simulation used to drive the control climate in this study

The GCM did not simulate the significant snowpack in the Sierra Nevada region because the model terrain could not capture the mesoscale mountain range. Thus, downscaling of GCM-generated climate data to a spatial resolution suitable for regional-scale features is an essential step in the climate change impact assessment (Giorgi et al. 1994; Kim et al. 2002; Cayan et al. 2008). Spatial downscaling of GCM data employs either statistical (e.g., Wood et al. 2002, 2004) or dynamical (e.g., Giorgi et al. 1994; Leung and Ghan 1999; Kim et al. 2002) methods. Both methods have their own advantages and drawbacks. For example, statistical downscaling has been widely used in surface hydrological applications (e.g., Gershunov and Cayan 2003; Wood et al. 2002); it is relatively inexpensive in terms of computational resources to perform, but the physical and dynamical consistency among the downscaled variables is not guaranteed. Moreover, in climate change projections, validity of the method relies on an assumption that the relationship between the predictors and the predictands derived from the historical data is also valid in future climate. Compared to a statistical downscaling method, dynamical downscaling using an RCM is computationally much more expensive, but it can preserve the physical and dynamical consistencies among the downscaled variables. In addition, simulation skill varies significantly among RCMs, often resulting in large differences between the downscaled variables based on different RCMs (Duffy et al. 2006). Despite its current shortcomings, rapid progress in model formulations and faster computers makes dynamical downscaling an important tool for generating future climate data for regional impact assessment efforts.

This study investigates the impact of the climate change associated with increased GHGs on the surface hydroclimate in California by dynamically downscaling a global climate scenario generated by the NCAR CCSM3 on the basis of the Intergovernmental Panel on Climate Change (IPCC) SRES-A1B emission profile. Details on the experiment are presented in Section 2. Sections 3 through 6 present the climate change signals in the key surface hydroclimate during the cold season. Summary and conclusions are presented in Section 7.

2.0 Experiment

The dynamical downscaling was performed using the Weather Research and Forecast (WRF) model, version 2.2.1 (Skamarock et al. 2005). The model solves a non-hydrostatic momentum equation in conjunction with a thermodynamic energy equation. Numerically, the model features multiple options for the advection scheme and the parameterized atmospheric physical processes. In conjunction with one-way and/or interactive self-nesting capability, this allows us to apply the model to simulate atmospheric circulation of a wide range of spatial scales. More details of the WRF model can be found in the website <http://wrf-model.org>. The physics options selected in this experiment includes the NOAH land-surface scheme (Chang et al. 1999), the simplified Arakawa Schubert (SAS) convection scheme (Hong and Pan 1998), the rapid radiative transfer model (RRTM) longwave radiation scheme (Mlawer et al. 1997), Dudhia (1989) shortwave radiation, and the WSM 3-class with simple ice cloud microphysics scheme. For more details on the physics options, readers are referred to the website <http://wrf-model.org>.

The model domain covers the western United States at a 36 km horizontal resolution (Figure 2) and has 28 atmospheric and 4 soil layers in the vertical.

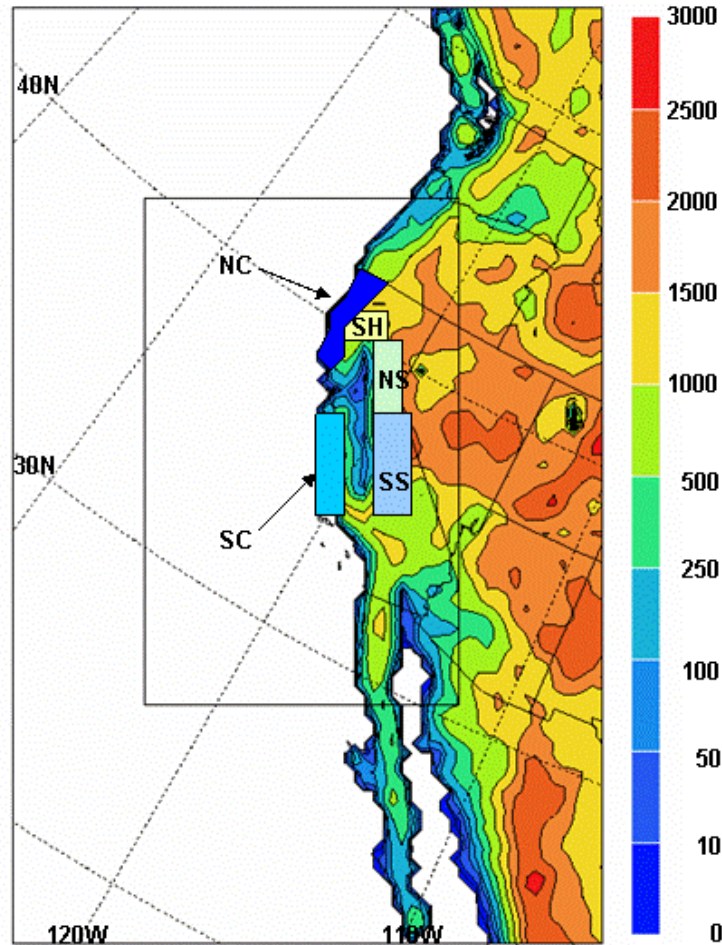


Figure 2. The model terrain (m) of the 36 km resolution western U.S. domain (outer box). The inner box represents the area where the climate signals obtained for this study are presented. The five California sub-regions are marked by colored rectangles.

Also shown in Figure 2 are the five sub-regions selected according to precipitation characteristics (Table 1). Among these sub-regions, the three regions SH, NS, and SS feed most of major reservoirs that supply water in California.

Table 1. Precipitation characteristics in the five California sub-regions in Figure 2

Region	Elevation Range	Rainfall	Snowfall
Northern Coastal Range (NC)	0–1500 m	Heavy	Light
Southern Coastal Range (SC)	0–1000 m	Heavy	Insignificant
Mt. Shasta (SH)	500–1500 m	Heavy	Heavy
Northern Sierra Nevada (NS)	500–2000 m	Heavy	Heavy
Southern Sierra Nevada (SS)	500–3000 m	Heavy	Heavy

The regional climate simulations are driven by the global climate data generated by the NCAR CCSM3 according to the SRES-A1B emission scenario (Nakicenovic et al. 2000) that assumes balanced energy generation between fossil and non-fossil fuel. The resulting carbon dioxide (CO₂) emissions are located near the averages of all *Special Report on Emissions Scenarios* (SRES) emissions scenarios; perhaps representative for many possible emission scenarios. This is one of the reasons behind the selection of the scenario in this study. Due to the limitation in computational resources and the availability of the GCM datasets suitable for dynamical downscaling, this study is limited to the single emissions scenario. The climatology for the late twentieth century and mid-twenty-first century periods is calculated from the 20 cold season (October–March) regional simulations for 1961–1980 and 2035–2054, respectively. The CO₂ concentrations in the WRF simulations are fixed at 330 parts per million, volume (ppmv) and 430 ppmv during the present-day and mid-twenty-first century periods, respectively. Figure 3 presents a schematic illustration of the data flow in the downscaling. Individual runs were initialized at 00 coordinated universal time (UTC) October 1 of the corresponding years using the CCSM-3 output data. All simulations are continued for the remaining six-month period without reinitialization by updating the large-scale forcing along the lateral boundaries at three-hour intervals.

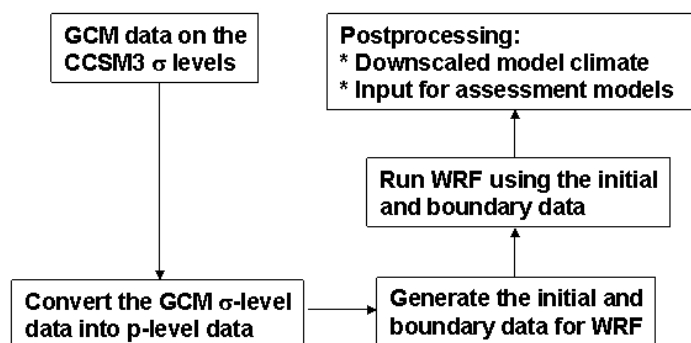


Figure 3. The information flow in the experiment

In the following, the impact of the anthropogenic climate change on the key surface hydroclimate fields in the California region is presented in terms of the climate change signals. The climate change signal in a variable is defined as the difference in the 20-year climatology of the variable between the mid-twenty-first century and the mid-twentieth century periods. The hydroclimate fields examined in this study include the near-surface air temperature, precipitation, rainfall, snowfall, runoff, snowmelt, and snowpack—which play crucial roles in shaping water resources, hydropower generation, and ecosystems in the region.

3.0 The Changes in the Low-Level Air Temperature

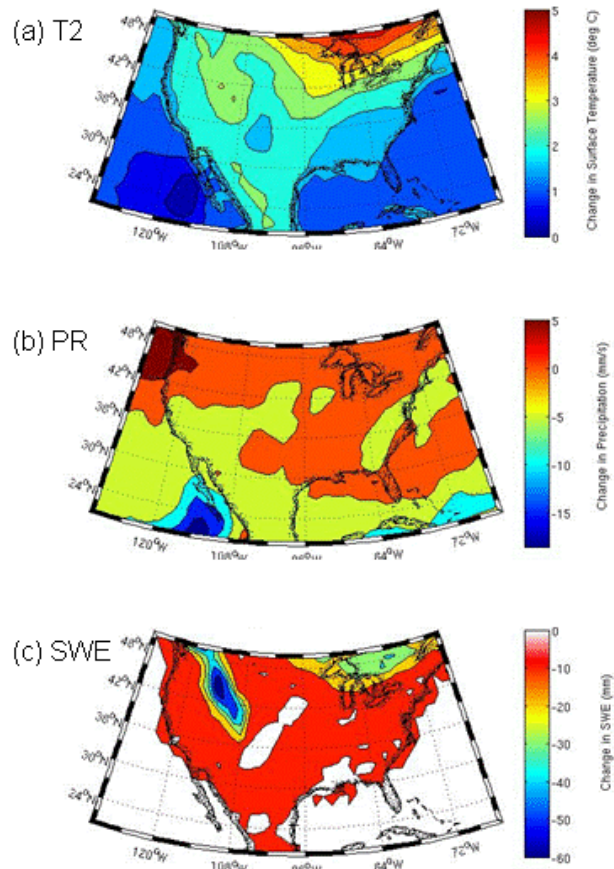


Figure 4. The CCSM3-projected climate change signals in the (a) low-level air temperature, (b) precipitation, and (c) SWE during the cold season

Figure 4 presents the climate change signals calculated from the CCSM3 simulation for the same periods that are downscaled in this study. The GCM projection shows a warming of 1°C–2°C (1.8°F–3.6°F) over California and most of the Pacific coast regions (Figure 4a). The GCM also projects decrease of cold season precipitation to the south of the Northern California region, and increases in the region to the north of it (Figure 4b). The projected SWE decreases everywhere; however, the only meaningful signals are generated over the Rocky Mountain region (Figure 4c) because the GCM could not resolve the significant mesoscale orography in the Pacific coast region. The climate change signals obtained in the downscaled projection are presented below.

Increases in the low-level air temperatures by 1°C–2.5°C (1.8°F–4.5°F) in California (Figure 5a) are projected for the entire cold season (October–March). The warming signals are largest in the high-elevation regions in the Sierra Nevada and are smallest in the coastal regions and in the Central Valley. The projected warming signals are similar (in spatial pattern and magnitude) to the results in previous studies for the region on the basis of various global and regional climate models (Giorgi et al. 1994; Kim et al. 2002; Leung et al. 2004; Duffy et al. 2006). The strong

gradient in the warming signal between the coastal and mountain/inland regions results chiefly from two factors: (1) the prevailing westerly winds advecting the relatively colder maritime air into the land during the cold season, and (2) the reduction in surface albedo associated with smaller snow cover in the high-elevation regions in the warmer climate, as discussed in previous studies (e.g., Kim et al. 2002). The contribution of these two effects to the spatial variations in the warming signal could not be quantified separately because the temperature change signal results from complex interaction between the advection and local physical feedback. Note that general features in seasonal wind field remain similar in the two time periods (not shown). The downscaled temperature signal is similar to that in the GCM projection above, but it contains more details, especially in showing local terrain variations.

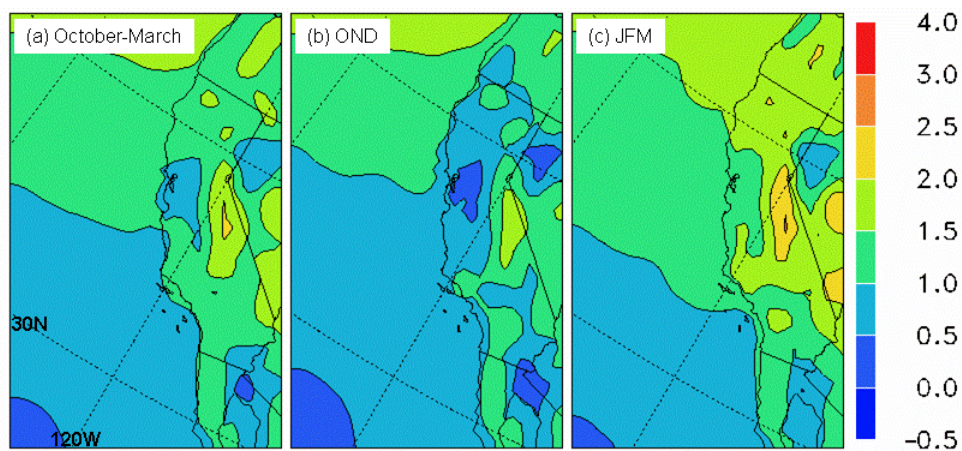


Figure 5. The low-level temperature change signals for: (a) the entire cold season (October–March), (b) fall (October–December: OND), and (c) winter (January–March: JFM)

The projected low-level temperature changes show noticeable differences between the early (fall: OND) and the late (winter: JFM) cold season (Figure 5b,c). The downscaled temperature signals in the California region are as large as 2°C (3.6°F) for fall with larger increases in the southeastern California region (Figure 4b). Much larger temperature increases, 1.5°C–3°C (2.7°F–5.4°F), are projected for winter with the largest values over the Sierra Nevada and the southeastern part of the state (Figure 5c). The differences in the surface albedo between the mid-twenty-first century and the late twentieth century runs (Figure 6) reveal significant reduction in the surface albedo over high-elevation regions including the Sierra Nevada and the Mt. Shasta regions, especially in the later half of the cold season (JFM). The projected climate change signals in the low-level temperature and surface albedo shows that the link between the low-level temperature changes and the changes in surface albedo appears to be especially strong in high-elevation regions.

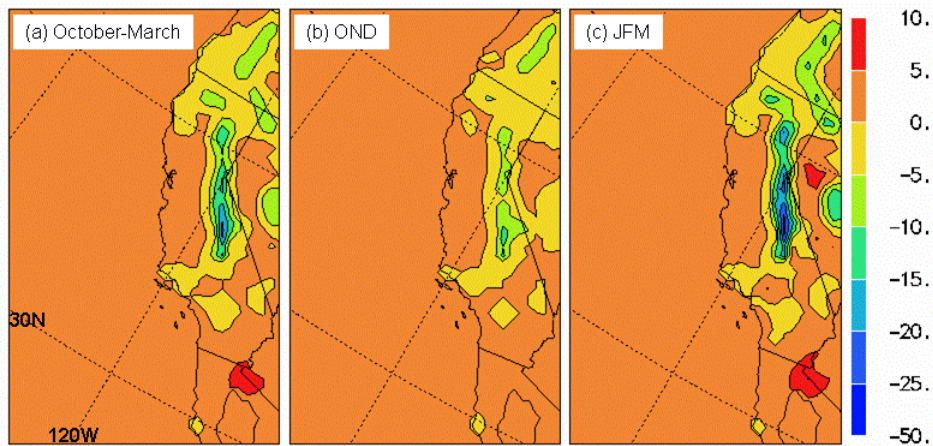


Figure 6. The percent changes in surface albedo for: (a) the entire cold season (October–March), (b) fall (OND), and (c) winter (JFM)

The low-level temperature changes within the five sub-regions in California (Table 2) show that the projected warming signal is larger in winter than in fall. Figure 2 shows the locations of the five sub-regions. The largest warming signals occur in the Mt. Shasta, northern Sierra Nevada, and southern Sierra Nevada regions during the later half of the cold season. These regions coincide with the areas in which the largest reduction in the surface albedo is projected (Figure 6). Thus, the large warming signals in these regions are, at least partially, related with the reduction in winter snowcover that resulted in increases in the surface solar forcing. In the coastal regions, warming over the northern Coastal Range is larger than over the southern Coastal Range for both fall and winter. These warming signals in the coastal regions may be related with the large-scale warming signals that generally increase towards the north, as can be inferred from the temperature change signals over the eastern Pacific Ocean (Figure 3). The reduction in the surface albedo may also contribute to the projected warming signals in the northern Coastal Range, especially during winter.

4.0 Precipitation Changes

The cold season precipitation in the RCM projection decreases in almost all regions in California in the warmer climate (Figure 7) consistently with the corresponding GCM projection (Figure 4b). The decrease in precipitation is most pronounced in the southern Coastal Range, the Sierra Nevada, and the southern California regions by 10%–25% of the amounts in the late twentieth century climate run. The significant decrease in cold season precipitation in the Sierra Nevada region is a serious concern because of its importance in California water resources. The spatial pattern of the precipitation change signals varies significantly between the early and late half of the cold season, especially in the north-south direction. In fall, the precipitation increases in the northern California region are accompanied by the decreases in the southern California region (Figure 7b). This spatial pattern in the fall precipitation change signals is reversed in winter; positive (negative) changes in the southern (northern) California region (Figure 7c).

Table 2. The projected climate change signals in key surface hydrologic variables within the five subregions (Table 1). The numbers in the parenthesis present the climate change in terms of the percent of the late twentieth century RCM climatology. The percent change in snowfall and snowmelt in the southern Coastal Range region (SC) is undefined, due to very small values in both the control and mid-century periods.

	Season	NC	SC	SH	NS	SS
Precip (mm/mo)	Fall	22.5 (11.5)	-6.6 (-11.7)	23.5 (15.2)	16.1 (9.85)	-16.0 (-15.4)
	Winter	-64.4 (-21.5)	-15.1 (-14.6)	-44.8 (-17.1)	-82.6 (-26.6)	-39.8 (-20.9)
	Oct–Mar	-21.0 (-8.46)	-10.9 (-13.6)	-10.7 (-5.12)	-33.2 (-14.0)	-27.9 (-19.0)
Rainfall (mm/mo)	Fall	25.4 (13.5)	-6.7 (-12.2)	34.8 (28.0)	29.6 (22.7)	-3.6 (-5.1)
	Winter	-54.7 (-19.4)	-15.5 (-15.0)	-14.0 (-6.93)	-45.8 (-19.1)	-12.2 (-10.7)
	Oct–Mar	-14.6 (-6.23)	-11.2 (-14.0)	10.4 (6.4)	-8.1 (-4.4)	-7.9 (-8.6)
Snowfall (mm/mo)	Fall	-2.9 (-41.7)	0.2 (n/a)	-11.3 (-38.0)	-13.5 (-40.5)	-12.5 (-36.5)
	Winter	-9.7 (-53.1)	0.4 (n/a)	-30.8 (-51.3)	-36.8 (-52.6)	-27.6 (-36.5)
	Oct–Mar	-6.3 (-50.0)	0.3 (n/a)	-21.1 (-46.9)	-25.1 (-48.7)	-20.0 (-36.5)
Runoff (mm/mo)	Fall	-0.1 (-0.4)	-0.2 (-11.7)	0.7 (5.6)	-1.9 (-10.7)	-6.5 (-63.1)
	Winter	-12.9 (-10.4)	-3.4 (-28.2)	-3.6 (-3.8)	-24.9 (-22.6)	-16.5 (-29.4)
	Oct–Mar	-6.5 (-8.6)	-1.78 (-26.7)	-1.4 (-2.7)	-13.4 (-21.0)	-11.5 (-34.6)
Snowmelt (mm/mo)	Fall	-2.89 (-42.6)	0.2 (n/a)	-10.1 (-36.4)	-11.3 (-37.7)	-8.5 (-29.9)
	Winter	-9.75 (-52.8)	0.4 (n/a)	-32.3 (-51.9)	-39.4 (-54.0)	-30.7 (-38.6)
	Oct–Mar	-6.32 (-50.0)	0.3 (n/a)	-21.2 (-47.2)	-25.4 (-49.2)	-19.6 (-36.3)
SWE (mm)	Fall	0.1 (42.3)	0.0 (0.0)	-1.1 (-32.9)	-1.4 (-29.9)	-3.1 (-42.7)
	Winter	-1.3 (-78.5)	0.0 (0.0)	-2.9 (-58.1)	-5.0 (-65.5)	-13.2 (-67.9)
	Oct–Mar	-0.6 (-60.8)	0.0 (0.0)	-2.0 (-47.7)	-3.21 (-52.0)	-8.2 (-61.1)
2m air temperature (°C)	Fall	0.87	0.59	0.95	0.98	1.38
	Winter	1.73	1.42	1.77	1.94	2.09
	Oct–Mar	1.30	1.00	1.36	1.46	1.74

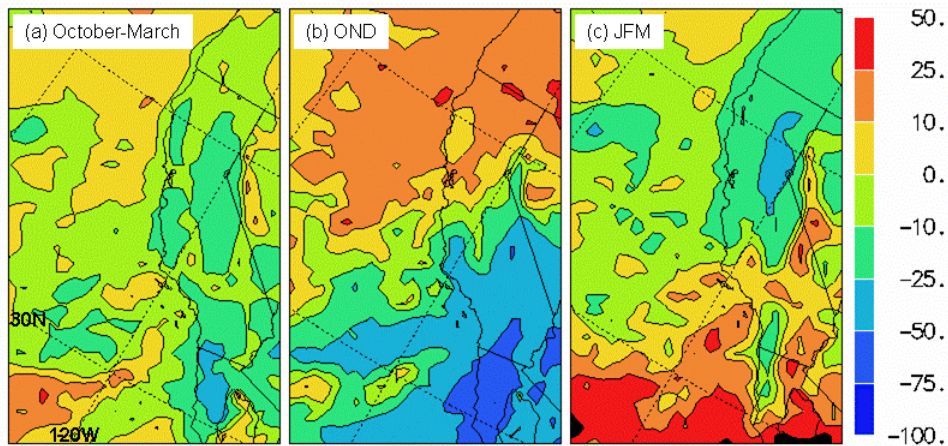


Figure 7. The climate change signal in precipitation (percent of the control climate) for: (a) the entire cold season (October–March), (b) fall (OND), and (c) winter (JFM)

The differences in rainfall and snowfall between the late twentieth century and the mid-twenty-first century are further examined below. The results show that the cold season rainfall decreases generally in California except in high-elevation regions in the Sierra Nevada, where the projected rainfall increases are as large as 25% of the values in the late twentieth century climate condition (Figure 8). The largest decrease in cold season rainfall occurs in the southern Coastal Range, the Central Valley, and the southern California regions by 10%–25% of the values in the late twentieth century run. Seasonally, the spatial pattern of the projected rainfall changes in California closely resembles the seasonal precipitation changes of Figure 7. Important differences between the seasonal precipitation and rainfall changes appear in the northern Sierra Nevada region during fall; fall rainfall (Figure 8b) increases in the region despite the decrease in precipitation (Figure 7b). This is because the reduction in fall snowfall (Figure 9b) is much larger than the increase in rainfall in this region.

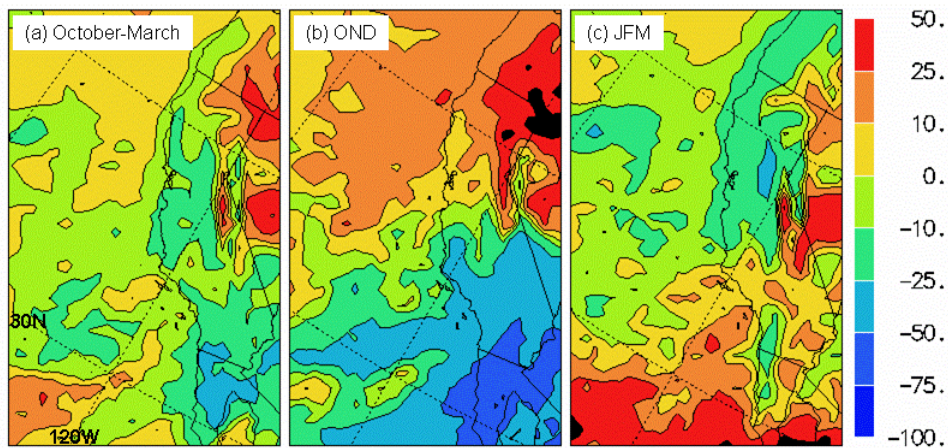


Figure 8. Same as Figure 5, but for the seasonal rainfall changes

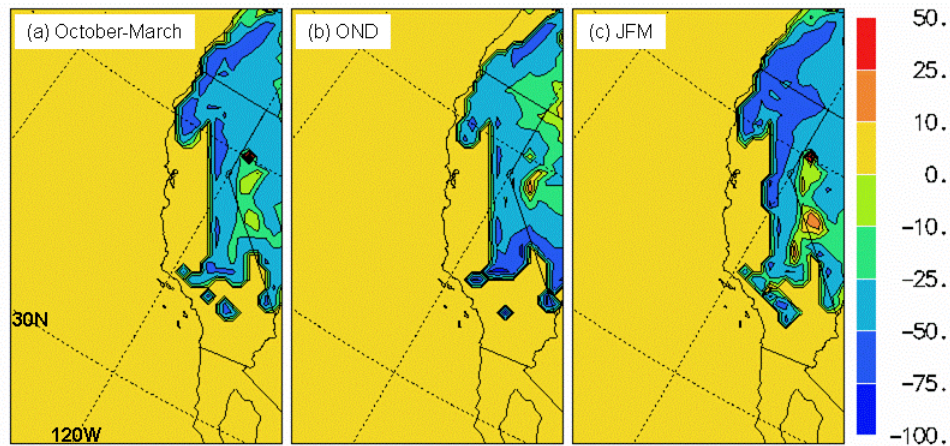


Figure 9. Same as Figure 5, but for the seasonal snowfall changes

The projected mid-twenty-first century snowfall decreases by 25%–50% of the late twentieth century values in the Sierra Nevada region and by over 50% in the Mt. Shasta region (Figure 9). This is one of important consequences of the low tropospheric warming which results in higher freezing level altitudes during storms (Giorgi et al. 1997; Kim 2001). The snowfall over the Sierra Nevada decreases by similar percentages for both fall and winter; however, the snowfall decreases in the Mt. Shasta region are much larger in winter than in fall (not shown).

The climate change signals in the seasonal precipitation, rainfall, and snowfall in the five California sub-regions are also summarized in Table 2. Precipitation and rainfall increases during fall in the three northern regions: the northern Coastal Range, Mt. Shasta, and the northern Sierra Nevada. The increase in fall precipitation and rainfall in these regions are followed by decreases during the winter, resulting in net decreases in precipitation and rainfall over the entire cold season. Note that Figures 5–7 present the climate change signals in terms of the percentage of the amounts in the control climate. Because precipitation amounts are much larger in winter than in fall (not shown), the precipitation changes over the entire cold season are dominated by the changes in winter. In the two southern regions, the southern Coastal Range and the southern Sierra Nevada, precipitation and rainfall decreases for both fall and winter. Snowfall decreases in all regions except in the southern Coastal Range region, where snowfall is insignificant.

5.0 The Changes in the Seasonal Snowpack and Snowmelt

The projected seasonal-mean snow water equivalent (SWE) decreases in the high-elevation regions in California (Figure 10). The significant reduction in SWE during winter is alarming because the amount of snowpack in high-elevation regions at the end of winter is a key indicator for warm season water supply in California. The projected SWE decreases in the three northern regions are about 30%–40% in fall and almost 60%–80% in winter (Table 2). For the entire cold season, the SWE reduction is almost as large as the amounts in the present-day condition. The decrease in SWE is consistent with the significant decrease in snowfall and may

be augmented by increased melting due to warmer low-level temperature. The reduction in SWE for both seasons is consistent with the reduction of the surface albedo in the mountainous regions in California, as shown in Figure 6.

The snowmelt in the three sub-regions decreases throughout the cold season in response to the reduced snowfall in the warmer climate (not shown). The largest reduction occurs in the northern Sierra Nevada region (Table 2) where the snowmelt decreases by 38% and 54% of the late twentieth century values for fall and winter, respectively. The percent change in the projected snowmelt reduction in the Mt. Shasta region is similar to that in the northern Sierra Nevada region. In the southern Sierra Nevada region, the amount of snowmelt change remains somewhat smaller than the amount of changes in the Mt. Shasta and the northern Sierra Nevada regions for both fall and winter because the low-level air temperature remains lower than other regions in this high-elevation region, as discussed in Kim (2001).

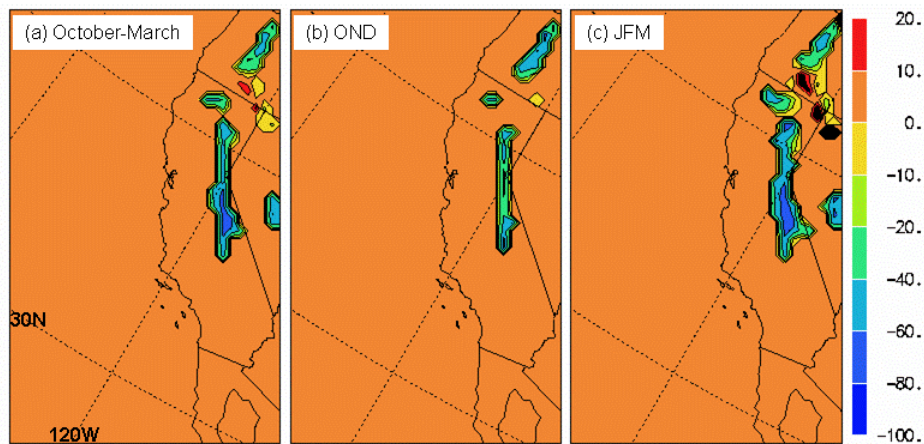


Figure 10. The climate change signals (% of the control climate) in SWE for: (a) the entire cold season, (b) fall, and (c) winter

6.0 Runoff Changes

The projected runoff decreases in all five sub-regions for both fall and winter, except in the Mt. Shasta region, where runoff increases slightly in fall in response to the slight increase in fall rainfall (Table 2). In the three northern California regions (the northern Coastal Range, Mt. Shasta, and the northern Sierra Nevada) runoff changes show large seasonal variations with smaller decreases in fall and larger decreases in winter. In these northern regions, the increase in fall precipitation and rainfall partially compensates the decrease in fall snowfall to result in a relatively small amount of fall runoff reduction. In the two southern regions, the southern Coastal Range and the southern Sierra Nevada, significant reduction in seasonal runoff is projected for the both seasons in response to the decrease in precipitation throughout the cold season. The amount of runoff change is smallest in the Mt. Shasta region and largest in the southern Sierra Nevada region (Table 2).

7.0 Summary and Conclusions

The impact of the global climate change induced by anthropogenic forcings, especially the increase in the atmospheric GHG, on the cold season surface hydroclimate in California in the mid-twentieth century has been investigated using the dynamical downscaling method. In the present study, the WRF model is driven by the six-hourly large-scale atmospheric and sea surface temperature (SST) forcing from a CCSM3 global climate projection based on the SRES-A1B emission scenarios to obtain regional-scale climate data at a 36 km horizontal resolution. The cold season includes fall and winter in this study. The climate change signals of key hydroclimate fields are calculated as the difference in the 20-year climatology between 2035–2054 and 1961–1980.

The regional climate change signals obtained in this study show that;

1. The low-level air temperature will increase by 1°C–2.5°C (1.8°F–4.5°F), with larger increases in high-elevation regions during the late half of the cold season. The geographical variations in the warming signals are associated with the effects of the significant depletion of snowpack in the warmer climate and the prevailing westerlies.
2. Surface albedo decreases notably in high-elevation regions in northern California and the Sierra Nevada. The decrease in the surface albedo is more pronounced in winter than in fall because of a larger depletion of snowpack in winter.
3. The cold season precipitation decreases in the entire region of California. The precipitation changes show strong interseasonal variations: Fall precipitation increases in the northern California region and decreases in the southern California region. The winter precipitation changes show opposite features with increases (decreases) in the southern (northern) California region.
4. Winter rainfall changes are similar to those in precipitation. Rainfall increases notably in the high-elevation regions in the northern Sierra Nevada, where a significant portion of snowfall in the present-day climate falls as rain in the warmer climate due to higher freezing level altitudes.
5. Snowfall decreases for all seasons by 25%–50% of the amounts in the present-day climate. The largest percent-decrease in snowfall occurs in the Mt. Shasta and the northern Sierra Nevada regions during the second half of the cold season (winter).
6. The snowpack in the high-elevation Mt. Shasta and the Sierra Nevada regions decreases by over 40% in fall and nearly 70% in winter due to reduced snowfall. The reduced snowfall in the warmer climate also results in the reduction in snowmelt by 38% and 54% of the late twentieth century values during fall and winter, respectively.
7. The cold season runoff decreases in California due to reduced precipitation.

The climate change signals obtained in this study suggest that climate change will adversely affect California's water resources. The projected decrease in snowfall and snowpack is of special concern because snowpack in high-elevation regions plays a role of natural reservoir

that stores water during the wet, cold season and gradually releases it through the early part of the dry, warm season.

It must be noted that the results presented in this study represent only one of many equally plausible scenarios. The changes in the key surface hydroclimate fields projected in this study compare qualitatively with the results in previous studies (Leung and Ghan 1999; Kim et al. 2002); however, details in the projected climate change signals vary among these studies. Further examinations reveal that major differences in the climate change signals projected in this and previous studies, especially the changes in regional precipitation, are primarily due to the differences in the GCM climate projections used in each regional climate change study. For example, the previous study by Kim et al. (2002) projected cold season precipitation increases in the northern California region, an opposite to the projections obtained in the present study. Their results are directly related to the precipitation signal projected by the GCM used to drive the simulation. Other studies based on NCAR GCM projections (e.g., Leung and Ghan 1999) tend to predict decreases in cold season precipitation as in this study; in this and their studies, the corresponding the GCM scenarios also project decreased precipitation. In regional climate modeling studies for Europe, Schmildi et al. (2002) and Déqué et al. (2007) also found that the largest uncertainties in the downscaled precipitation is associated with the differences in the large-scale circulation among GCMs. The strong dependence of regional climate change projections on the driving GCM, especially precipitation in California, is due to the fact that the most crucial factor that determines the precipitation in California, the water vapor flux from the Pacific Ocean, for the regional model domain is almost entirely determined by the GCM projection. Considering the large uncertainty in projecting regional climate change signals due to GCM scenarios, it is necessary to expand this study to include climate scenarios from multiple GCMs in order to better quantify the range of uncertainties in the regional climate change signals.

8.0 References

- Anderson, J., F. Chung, M. Anderson, L. Brekke, D. Easton, M. Ejeta, R. Peterson, and R. Snyder. 2008. "Progress on incorporating climate change into management of California's water resources." *Climatic Change* 87:S91–S108.
- Cayan, D., E. Maurer, M. Dettinger, M. Tyree, and K. Hayhoe. 2008. "Climate change scenarios for the California region." *Climatic Change* 87:S21–S42.
- Chang, S., D. Hahn, C. Yang, D. Norquist, and M. Ek. 1999. "Validation study of the CAPS model and land surface scheme using the 1987 Cabauw/PILPS dataset." *J. Appl. Meteor.* 38:405–422.
- Dettinger, M., and D. Cayan. 1995. "Large-scale atmospheric forcing of recent trends toward early snowmelt runoff in California." *J. Climate* 8:606–623.

- Déqué, M., D. Rowell, D. Lüthi, F. Giorgi, J. Christensen, B. Rockel, D. Jacob, E. Kjellström, M. de Castro, and B. van den Hurk. 2007. "An intercomparison of regional climate simulations for Europe: assessing uncertainties in model projections." *Climatic Change*, doi:10.1007/s10584-006-9228-x.
- Dudhia, J. 1989. "Numerical study of convection observed during the winter monsoon experiment using a mesoscale two-dimensional model." *J. Atmos. Sci.* 46:3077–3107.
- Duffy, P., R. Arritt, J. Coquard, W. Gutowski, J. Han, J. Iorio, J. Kim, R. Leung, J. O. Roads, and E. Zeledon. 2006. "Simulations of present and future climates in the Western United States with four nested regional climate models." *J. Climate* 19:873–895.
- Gershunov, A., and D. Cayan. 2003. "Heavy daily precipitation frequency over the contiguous United States: Sources of climatic variability and seasonal predictability." *J. Climate* 16:2752–2765.
- Giorgi, F., C. S. Brodeur, and G. T. Bates. 1994. "Regional climate change scenarios over the United States produced with a nested regional climate model." *J. Climate* 7:375–399.
- Giorgi, F., J. W. Hurrell, M. R. Marinucci, and M. Beniston. 1997. "Elevation dependency of the surface climate signal: A model study." *J. Climate* 10:288–296.
- Hong, S., and H. Pan. 1998. "Convective trigger function for a mass flux cumulus parameterization scheme." *Mon. Wea. Rev.* 126:2599–2620.
- IPCC. 1995. *Climate Change 1995 – The Science of Climate Change*. Intergovernmental Panel on Climate Change, WMO. 572 pp.
- IPCC. 2000. *Emissions Scenarios*. A Special Report of IPCC Working Group III. ISBN: 92-9169-113-5, 20 pp.
- IPCC. 2007. *Climate Change 2007 – Synthesis Report*. Intergovernmental Panel on Climate Change, WMO 73 pp.
- Kim, J. 2001. "A nested modeling study of elevation-dependent climate change signals in California induced by increased atmospheric CO₂." *Geophys. Res. Lett.* 28:2951–2954.
- Kim, J., T. Kim, R. W. Arritt, and N. Miller. 2002. "Impacts of increased atmospheric CO₂ on the hydroclimate of the Western United States." *J. Climate* 15:1926–1942.
- Kim, J., and J. Lee. 2003. "A multiyear regional climate hindcast for the western United States using the Mesoscale Atmospheric Simulation model." *J. Hydrometeorol.* 4:878–890.
- Kim, J. 2004. "A projection of the effects of the climate change induced by increased CO₂ on extreme hydrologic events in the western U.S." *Climatic Change* 68:153–168.
- Kyriakidis, P., J. Kim, and N. Miller. 2001. "Geostatistical mapping of precipitation using atmospheric and terrain characteristics." *J. Appl. Meteor.* 40:1855–1877.

- Leung, L., and S. Ghan. 1999. "Pacific Northwest climate sensitivity by a regional climate model driven by a GCM. Part II: 2 x CO₂ simulations." *J. Climate* 12:2031–2053.
- Leung, R., Y. Qian, X. Bian, W. Washington, J. Han, and J. O. Roads. 2004. "Mid-century ensemble regional climate change scenarios for the Western United States." *Climatic Change* 62:75–113.
- Mlawer, E., S. Taubman, P. Brown, M. Iacono, and S. Clough. 1997. "Radiative transfer for inhomogeneous atmosphere: RRTM, a validated correlated-k model for the longwave." *J. Geophys. Res.* 102:16663–16682.
- Nakicenovic, N., and coauthors. 2000. *Special Report on Emissions Scenarios*. IPCC Special Report, Nakicenovic, N., and R. Swart (Eds.). Cambridge University Press. 570 pp.
- Schmildi, J., C. Schmutz, C. Frei, H. Wanner, and C. Schär. 2002. "Mesoscale precipitation variability in the region of the European Alps during the 20th century." *International J. of Climatology*. 22:1049-1074. Doi:10.1002/joc.769.
- Skamarock, W., J. Klemp, J. Dudhia, D. Gill, D. Baker, W. Wang, and J. Powers. 2005. *A description of the advanced research WRF version 2*. NCAR/TN-468+STR. 88pp.
- Stewart, I., D. Cayan, and M. Dettinger. 2005. "Changes towards earlier streamflow timing across western North America." *J. Climate* 18:1136–1155.
- Wood, A., E. Maurer, A. Kumar, and D. Lettenmaier. 2004. "Long-range experimental hydrologic forecasting for the eastern United States." *J. Geophys. Res.* 107:4429.
- Wood, A., L. Leung, V. Sridhar, and D. Lettenmaier. 2004. "Hydrological implications of dynamical and statistical approaches to downscaling climate model outputs." *Climatic Change* 62:189–216.

9.0 Glossary

CCM3	NCAR Community Climate Model
CO ₂	carbon dioxide
GCM	global climate model
GHG	greenhouse gas
HadCM2	Hadley Centre Climate Model
IPCC	Intergovernmental Panel on Climate Change
JFM	January, February, March
JIFRESSE	Joint Institute for Regional Earth System Science and Engineering

JPL	Jet Propulsion Laboratory
MAS	Mesoscale Atmospheric Simulation model
NAS	NASA Advanced Supercomputing division
NASA	National Aeronautics and Space Administration
NCAR	National Center for Atmospheric Research
OND	October, November, December
RCM	regional climate model
RRTM	rapid radiative transfer model
SAS	Arakawa Schubert convection scheme
SRES	<i>Special Report on Emissions Scenarios</i>
SST	sea surface temperature
SWE	snow water equivalence
UTC	coordinated universal time
WRF	Weather Research and Forecast